Journal of Photochemistry and Photobiology A: Chemistry 201 (2009) 228–236

Contents lists available at ScienceDirect

Journal of Photochemistry and Photobiology A: Chemistry

journal homepage: www.elsevier.com/locate/jphotochem

Opposing responses elicited by positively charged phthalocyanines in the presence of CdTe quantum dots

Sharon Moeno, Tebello Nyokong*

Department of Chemistry, Rhodes University, Grahamstown 6140, South Africa

ARTICLE INFO

Article history:
Received 3 July 2008
Received in revised form 28 October 2008
Accepted 31 October 2008
Available online 21 November 2008

Keywords:
Quantum dots
Mercaptopropionic acid
Thioglycolic acid
Metallophthalocyanine
2-Mercaptopyridine
Energy transfer

ABSTRACT

Tetrapositively charged phthalocyanines and CdTe quantum dots (QDs) capped with thioglycolic acid (TGA) and mercaptopropionic acid (MPA) were synthesized. The response of the tetrapositively charged zinc phthalocyanines in the presence of quantum dots was studied. Aggregation and charge transfer were observed for [tetramethyl-2,(3)-[tetra-(2-mercaptopyridinephthalocyaninato)]zinc(II)]$^{4+}$ (TmTMPyZnPc), however aggregation proved to be the more prominent process of the two. Fluorescence resonance energy transfer (FRET) was observed with [tetramethyl-2,(3)-[tetra-(2-pyridyloxyphthalocyaninato)]zinc(II)]$^{4+}$ (TmTPyZnPc). In the FRET study the efficiency of FRET with TmTPyZnPc was determined to be 21% for both MPA and TGA capped CdTe QDs. For the charge transfer study the fluorescence of the quantum dots was quenched by the TmTMPyZnPc used, and from these quenching studies the quenching constants, binding constants and number of binding sites on the quantum dots were determined.

1. Introduction

In recent years quantum dots (QDs), which are nanometer sized semiconductor particles, have become a major field of interest in various branches of science [1–10]. They exhibit size-dependent physico-chemical properties such as tunable narrow emission spectrum, excellent photostability and broad excitation spectra [1–15]. All these properties allow for the exploitation of QDs in a variety of fields. Some fields of application of QDs include biological labeling, use in optoelectronic devices and they also have a potential for use in photodynamic therapy (PDT) [16–26].

QDs are highly photoluminescent with moderate fluorescence quantum yield values [1–3,6,11,27]. The organic molecules used for passivation are diverse and have varied functional groups which further aid in functionalizing the QD. The capping groups thus allow the nanoparticles to interact with the surrounding environment via either electrostatic, covalent, hydrophobic interactions or hydrogen bonding [5].

In this work, water soluble CdTe QDs which were capped with thioglycolic acid (TGA) and mercaptopropionic acid (MPA) were prepared and the responses to the addition of tetrapositively charged zinc metallophthalocyanines (ZnPcs) were studied. The tetrapositively charged metallophthalocyanines (ZnPcs) are [tetramethyl-2,(3)-[tetra-(2-mercaptopyridinephthalocyaninato)]zinc(II)]$^{4+}$ (TmTMPyZnPc, **4**) and [tetramethyl-2,(3)-[tetra-(2-pyridyloxyphthalocyaninato)]zinc(II)]$^{4+}$ (TmTPyZnPc, **6**) (Scheme 1). These complexes are tetra substituted and consist of a mixture of isomers which are not easy to separate [28].

A number of studies has shown that QDs can serve as near infrared (IR) energy donors to photosensitizers, e.g. metallophthalocyanines (MPcs). The photosensitizer can then accept this energy in a process known as fluorescence resonance energy transfer (FRET). FRET is a non-radiative energy transfer between the fluorescent donor and a suitable energy acceptor fluorophore [29–35]. On the other hand, QDs are also known to engage in charge transfer processes, some of which are spontaneous [36–38]. We have recently shown a spontaneous charge transfer from QDs to a positively charged porphyrazine where the benzene ring was substituted with a pyridine ring [38]. In this work ZnPcs were substituted with thiopyridine or oxopyridine groups.

2. Experimental

2.1. Materials

Thioglycolic acid 99%, tellurium powder (200 mesh, 99.8%), phthalimide, quinoline, 2-mercaptopyridine, 2-hydroxypyridine, chlorophyll a, 1,3-diphenylisobenzofuran (DPBF) and zinc acetate dihydrate were obtained from Sigma–Aldrich, sodium borohydride ($NaBH_4$), sodium hydroxide (NaOH), sulphuric acid (H_2SO_4), potassium carbonate (K_2CO_3), ferric chloride ($FeCl_3$), nitric acid (HNO_3), ethanol, tetrahydrofuran (THF), chloroform ($CHCl_3$),

* Corresponding author. Tel.: +27 46 6038260; fax: +27 46 6225109.
E-mail address: t.nyokong@ru.ac.za (T. Nyokong).

1010-6030/$ – see front matter © 2008 Elsevier B.V. All rights reserved.
doi:10.1016/j.jphotochem.2008.10.027

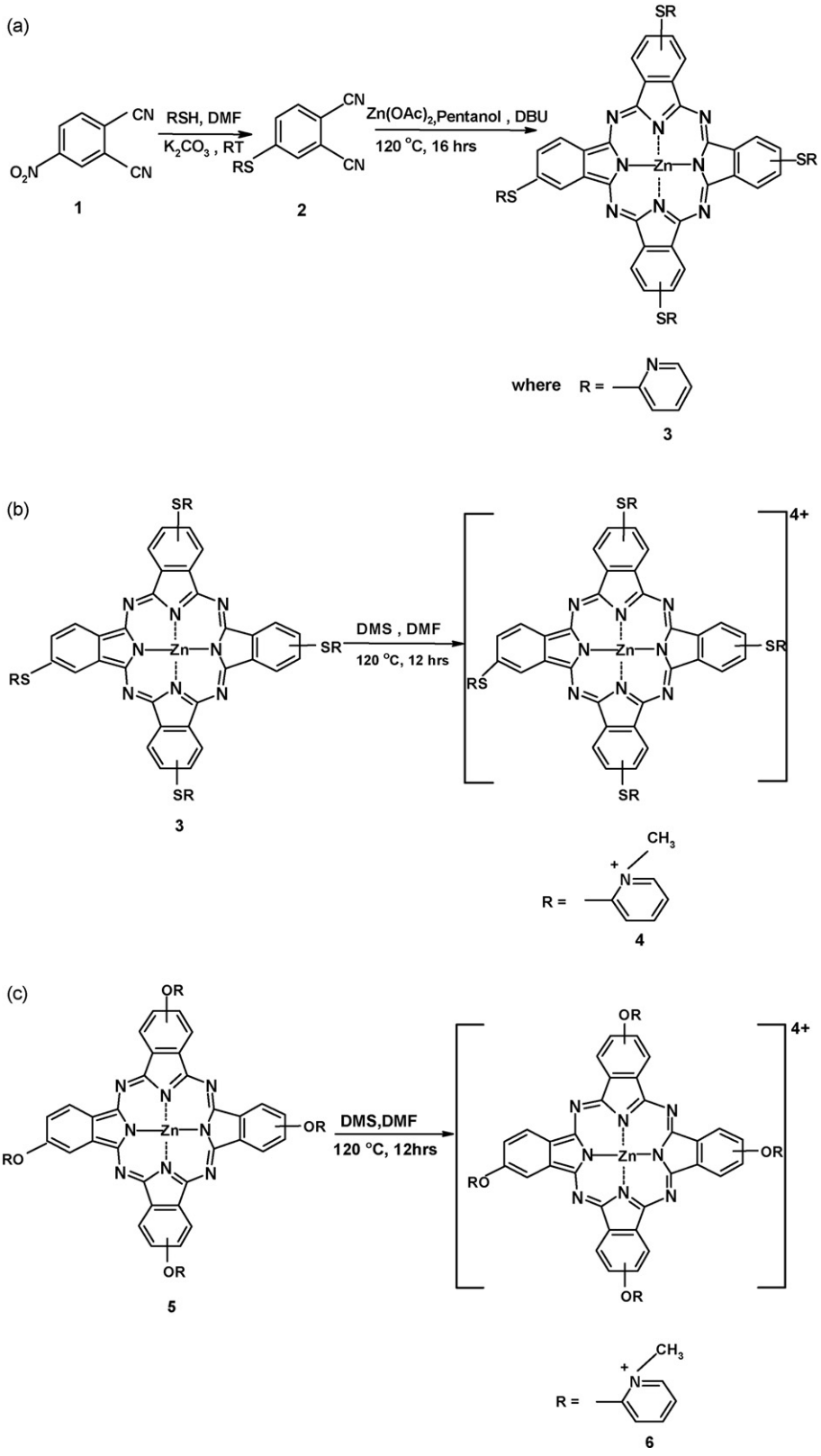

Scheme 1. Synthetic route of (a) 2-mercaptopyridine tetra substituted zinc(II) phthalocyanine (TmTMPyZnPc) complex, (b) quaternized 2-mercaptopyridine tetra substituted zinc(II) phthalocyanine (TmTMPyZnPc) complex and (c) quaternized 2-pyridyloxy tetra substituted zinc(II) phthalocyanine (TmTPyZnPc) complex.

hexane, diethyl ether, acetone, and dimethylformamide (DMF) were obtained from Saarchem. Pyridine, dimethyl sulphoxide and 1,8-diazabicyclo[5,4,0]undec-7-ene (DBU) were obtained from Fluka and cadmium chloride monohydrate ($CdCl_2{\cdot}H_2O$) and dimethyl sulphate (DMS) were obtained from Merck. Ultra pure water was obtained from a Milli-Q Water System (Millipore Corp., Bedford, MA, USA). A 50/50 pyridine:H_2O solution was employed for photophysical studies. This solvent mixture allows

for both QDs and MPc to dissolve while the monomerizing MPc complexes.

2.2. Synthesis

2.2.1. ZnPc derivatives

The syntheses of the phthalonitriles 4-(2-mercaptopyridine) phthalonitrile [39] and 4-(2-pyridyloxy)phthalonitrile [28,40] have been reported before. The synthesis of complex **5** (2,(3)-tetra-(2-pyridyloxy)phthalocyaninato)zinc(II) has also been reported before [40].

*2.2.1.1. (2,(3)-Tetra-(2-mercaptopyridine)phthalocyaninato)zinc(II) (**3**, Scheme 1a).* This complex was prepared according to a method previously reported for the MnPc derivative [39]. A mixture of anhydrous zinc(II) acetate (0.6 g, 2.8 mmol), 4-(2-mercaptopyridine)phthalonitrile (**2**) (0.5 g, 2.1 mmol), DBU (1.66 mL, 12 mmol) and quinoline (10 mL, doubly distilled over CaH_2) was stirred at 120 °C for 16 h under nitrogen atmosphere. After cooling, the solution was mixed with *n*-hexane. The blue solid product was precipitated and collected by filtration and washed with *n*-hexane. The crude product was re-dissolved in DMF. After concentrating, the blue product was precipitated with hot ethanol and filtered, then washed with ethanol, acetone, THF, $CHCl_3$, *n*-hexane and diethyl ether. The blue product was further purified by passing through a silica gel column with THF as eluent. Yield: 0.12 g (23%). UV/vis (DMSO), λ_{max} (nm) ($\log\varepsilon$): 688 (5.00), 622 (4.22), 365 (4.43); IR (KBr), ν_{max} (cm^{-1}): 3062 (ν_{Ar-H}), 1569, 1573 ($\nu_{C=C}$). ^1H NMR (600 MHz, DMSO–d_6), δ (ppm): 9.01–8.74 (m, 8H), 8.60–8.52 (m, 4H), 8.27–8.15 (m, 4H), 7.83–7.74 (m, 4H), 7.49 (m, 4H), 7.26 (m, 4H). Calc. for $C_{56}H_{46}N_{12}S_4Zn$: C 61.56; H 2.78; N 16.57; Found: C 61.45, H 2.72, N 16.52.

Complexes **3** and **5** were then quaternized for water solubility using established procedures [39] to form quaternized 2,(3)-tetra-(2-mercaptopyridinephthalocyaninato)zinc(II) (**4**, Scheme 1b) and quaternized 2,(3)-tetra-(2-pyridyloxyphthalocyaninato)zinc(II) (**6**, Scheme 1c). The characterization of quaternized derivatives has recently been reported [41].

2.2.2. Quantum dots

CdTe quantum dots were synthesized using wet chemical routes with TGA and MPA cappings using reported methods [3]. Briefly, $CdCl_2$ (0.22 g, 1.18 mmol) was dissolved in 65 mL of deionized water and 0.26 g (2.86 mmol) of TGA was added to the $CdCl_2$ solution. The pH of this precursor solution was adjusted to 11.5 with 1 M NaOH and left under a flow of nitrogen gas for half an hour. The solution of NaHTe was prepared by modified literature method [3] as follows: 0.05 M NaOH was reacted with H_2Te gas (the latter generated by reaction of $NaBH_4$ with Te powder in the presence of 0.5 M H_2SO_4 under a flow of nitrogen gas). Then the freshly prepared NaHTe (0.091 g, 0.60 mmol) was added to the precursor solution. The solution was then refluxed under air at 100 °C for different times. Precipitation of the QDs from the aqueous colloidal solution was achieved by using propan-2-ol.

The quantum dots sizes were estimated using a polynomial fitting function (Eq. (1)) derived in literature [42].

$$D = (9.8127 \times 10^{-7})\lambda^3 - (1.7147 \times 10^{-3})\lambda^2 + (1.0064)\lambda - 194.84 \quad (1)$$

where λ is the absorption maxima of the QDs.

The fitting function is not valid for sizes of quantum dots outside the size range of 1–9 nm [42]. It is valid in this work since as reported before [38] the quantum dots sizes are within this range.

2.3. Photophysical and photochemical studies

2.3.1. Interaction of ZnPc derivatives with QDs

The interaction of the ZnPc derivatives with QDs was studied by spectrofluorometry at room temperature. An aqueous solution of QDs (fixed concentration of 1 mg mL^{-1}) was titrated with varying concentrations (0–5.3 × 10^{-6} M) of the ZnPc derivatives. The QDs were excited at 500 nm and fluorescence recorded between 510 and 800 nm. The steady decrease in the fluorescence intensity of QDs with increase in ZnPc derivative concentration was noted and used in the determination of the binding constants and the number of binding sites (*n*) on QDs according to Eq. (2) [43–45]:

$$\log\left[\frac{F_0 - F}{F - F_\infty}\right] = \log k_b + n\log[\text{ZnPc}] \quad (2)$$

where F_0 and F are the fluorescence intensities of QDs in the absence and presence of ZnPc derivative, respectively, F_∞ the fluorescence intensity of QDs saturated with ZnPc derivative, k_b the binding constant, and n the number of binding sites on QDs. Plots of $\log[(F_0 - F)/(F - F_\infty)]$ against log[ZnPc] provided the values of n (from slope) and k_b (from the intercept). The changes in QD fluorescence intensity were related to ZnPc derivative concentrations by Eq. (3) [45]:

$$\frac{F_0}{F} = 1 + K[\text{ZnPc}] \quad (3)$$

where K represents the quenching constant, and F_0 and F are the fluorescence intensities of the QDs in the absence and presence of ZnPc, respectively.

2.3.2. Fluorescence quantum yield determinations

Fluorescence quantum yields (Φ_F) were determined by a comparative method [46] using Eq. (4):

$$\Phi_F = \Phi_{F(Std)}\frac{F A_{Std} n^2}{F_{Std} A n_{Std}^2} \quad (4)$$

where F and F_{Std} are the areas under the fluorescence curves of the MPc derivatives and the reference, respectively. A and A_{Std} are the absorbances of the sample and reference at the excitation wavelength, and n and n_{Std} are the refractive indices of solvents used for the sample and standard, respectively. ZnPc in DMSO was used as a standard, $\Phi_F = 0.20$ [47] for the determination of fluorescence quantum yields of the ZnPc derivatives in the pyridine:water solvent mixture. Rhodamine 6G in ethanol with $\Phi_F = 0.94$ was employed as the standard for the quantum dots [48,49]. The sample and the standard were both excited at the same relevant wavelength. The fluorescence quantum yields of the QDs are represented as $\Phi_{F(QD)}$ where QD represents TGA or MPA capped CdTe QDs, and for ZnPc complexes the Φ_F are represented as $\Phi_{F(ZnPc)}$ (where ZnPc represents TmTMPyZnPc (**4**), and TmTPyZnPc (**6**)). The determined fluorescence quantum yield values of the QDs were employed in determining their fluorescence quantum yields in the mixture with ZnPc derivatives ($\Phi_{F(QD)}^{Mix}$) using Eq. (5):

$$\Phi_{F(QD)}^{Mix} = \Phi_{F(QD)}\frac{F_{QD}^{Mix}}{F_{QD}} \quad (5)$$

where $\Phi_{F(QD)}$ is the fluorescence quantum yield of the QDs alone, and was used as standard, F_{QD}^{Mix} is the fluorescence intensity of QDs in the mixture (with ZnPc derivatives) when excited at the excitation wavelength of the QDs (500 nm) and F_{QD} is the fluorescence intensity of the QD alone at the same excitation wavelength.

Triplet quantum yields were determined using a comparative method, using Eq. (6):

$$\Phi_T^{Sample} = \Phi_T^{Std} \frac{\Delta A_T^{Sample} \varepsilon_T^{Std}}{\Delta A_T^{Std} \varepsilon_T^{Sample}} \quad (6)$$

where ΔA_T^{Sample} and ΔA_T^{Std} are the changes in the triplet state absorbance of the ZnPc derivatives and the standard, respectively. ε_T^{Sample} and ε_T^{Std} are the triplet state extinction coefficients for the ZnPc derivative and standard, respectively. Φ_T^{Std} is the triplet state quantum yield for zinc tetrasulfophthalocyanine (ZnTSPc) used as standard in aqueous solution, $\Phi_T^{Std} = 0.56$ [50]. Φ_T was also determined for the mixture of QDs and ZnPc derivatives and is represented as $\Phi_{T(ZnPc)}^{Mix}$ and the corresponding triplet lifetime as $\tau_{T(ZnPc)}^{Mix}$.

Quantum yields of internal conversion (Φ_{IC}) were obtained from Eq. (7). This equation assumes that only three processes (fluorescence, intersystem crossing and internal conversion) jointly deactivate the excited singlet state of the ZnPc derivatives.

$$\Phi_{IC} = 1 - (\Phi_F + \Phi_T) \quad (7)$$

2.3.3. Singlet oxygen quantum yields

The singlet oxygen quantum yield (Φ_Δ) determinations were carried out using an experimental set-up that is described in detail elsewhere [51]. In this work Φ_Δ values were determined using DPBF as a singlet oxygen quencher and chlorophyll a as a standard, and employing Eq. (8) for calculations of the Φ_Δ values:

$$\Phi_\Delta = \Phi_\Delta^{Std} \frac{W_{DPBF} I_{abs}^{Std}}{W_{DPBF}^{Std} I_{abs}} \quad (8)$$

where Φ_Δ^{Std} is the singlet oxygen quantum yield for the standard ($\Phi_\Delta^{Std} = 0.59$ in pyridine) [52] and W_{DPBF} and W_{DPBF}^{Std} are the DPBF photobleaching rates in the presence of the ZnPc derivatives under investigation and the standard (chlorophyll a), respectively. I_{abs} and I_{abs}^{Std} are the rates of light absorption by the ZnPc derivatives and the standard, respectively. The initial DPBF concentration used was kept the same for both the ZnPc derivatives and chlorophyll a. A molar extinction coefficient for DPBF at $\lambda = 417$ nm in pyridine of $\varepsilon = 27{,}500\ dm^3\ mol^{-1}\ cm^{-1}$ [53] was employed.

2.4. Determination of FRET parameters

FRET is a non-radiative energy transfer from a photoexcited donor fluorophore, after absorption of a higher energy photon, to an acceptor fluorophore of a different species which is in close proximity. FRET is highly dependent on the following parameters: the center-to-center separation distance between donor and acceptor (r), the degree of spectral overlap of the donor's fluorescence emission spectrum and the acceptor's absorption spectrum (J) [29,49]. The occurrence of FRET is made evident by a decrease of the donor photoemission accompanied by an increase in the acceptor's fluorescence. FRET efficiency (Eff) is determined experimentally from the fluorescence quantum yields of the donor in the absence ($\Phi_{F(QD)}$) and presence ($\Phi_{F(QD)}^{Mix}$) of the acceptor using Eq. (9) [29,49]:

$$Eff = 1 - \frac{\Phi_{F(QD)}^{Mix}}{\Phi_{F(QD)}} \quad (9)$$

FRET efficiency (Eff) is related to r (Å) by Eq. (10) [49]:

$$Eff = \frac{R_0^6}{R_0^6 + r^6} \quad (10)$$

where R_0 (the Förster distance, Å) is the critical distance between fluorophores of the donor and the acceptor molecules at which the efficiency of energy transfer is 50% and depends on the quantum yield of the donor (Eq. (11)) [49]:

$$R_0^6 = 8.8 \times 10^{23} \kappa^2 n^{-4} \Phi_{F(QD)} J \quad (11)$$

where κ^2 is the dipole orientation factor, n the refractive index of the medium, Φ_F the fluorescence quantum yield of the donor in the absence of the acceptor, and J is the Förster overlap integral, defined by Eq. (12):

$$J = \int f_{QD}(\lambda) \varepsilon_{ZnPc}(\lambda) \lambda^4 \ \partial\lambda \quad (12)$$

where f_{QD} is the normalized QD emission spectrum and ε_{ZnPc} is the molar extinction coefficient of ZnPc derivatives. In this case, it is assumed that κ^2 is 2/3; such assumption is often made for donor–acceptor pairs in a liquid medium, since their dipole moments are considered to be isotropically oriented during the excited state lifetimes. Although electrostatic interactions are anticipated between QDs and the sterically demanding phthalocyanine derivatives, the exact orientation of the ZnPc derivative with regard to the QD is not known with certainty. Various conformations can be attained by the phthalocyanine complex on the surface of QDs. For the perpendicular orientation of the ZnPc derivative on the QD some degree of movement of the donor/acceptor species is expected. As a result the isotropic dynamical average ($\kappa^2 = 2/3$) is more appropriate than the static isotropic average ($\kappa^2 = 0.476$) because the donor–acceptor pair is not rigid. λ is the wavelength of the acceptor, at the Q-band. FRET parameters were computed using the program PhotochemCAD [54].

2.5. Equipment

Fluorescence excitation and emission spectra were recorded on a Varian Eclipse spectrofluorometer. UV–vis spectra were recorded on a Varian 500 UV-Vis/NIR spectrophotometer. Laser flash photolysis experiments were performed with light pulses produced by a Quanta-Ray Nd:YAG laser providing 400 mJ, 90 ns pulses of laser light at 10 Hz, pumping a Lambda-Physik FL3002 dye (Pyridin 1 dye in methanol). Single pulse energy ranged from 2 to 7 mJ. The analyzing beam source was from a Thermo Oriel xenon arc lamp, and a photomultiplier tube was used as a detector. Signals were recorded with a digital real-time oscilloscope (Tektronix TDS 360). The triplet life times were determined by exponential fitting of the kinetic curves using the program OriginPro 7.5.

Photo-irradiations for photodegradation or singlet oxygen determination were performed using a General electric Quartz line lamp (300 W). A 600 nm glass cut off filter (Schott) and water were used to filter off ultraviolet and infrared radiations, respectively. An interference filter (Intor, 670 nm with a band width of 40 nm) was additionally placed in the light path before the sample. Light intensity was measured with a POWER MAX5100 (Molelectron detector incorporated) power meter and was found to be 1.25×10^{16} photons $s^{-1}\ cm^{-2}$ for singlet oxygen studies.

3. Results and discussion

3.1. Absorption and emission spectra

QDs grow through the Ostwald ripening process during the course of heating [30]. As they grow both the absorbance and the emission spectra shift to longer wavelengths. The MPA and TGA capped CdTe QDs had their first emission peak at 525 nm after 15 min of refluxing. MPA and TGA capped QDs were grown until their emission reached 640 nm (Fig. 1). The sizes of the TGA capped

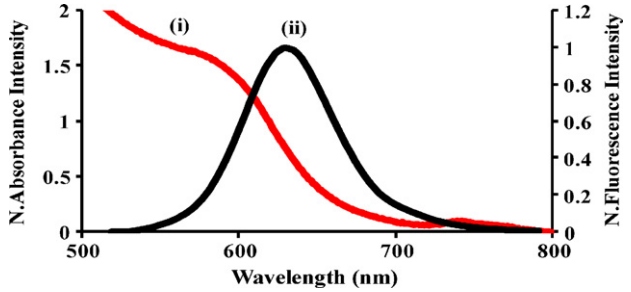

Fig. 1. Absorbance (i) and emission (ii) spectra of CdTe-TGA (1 mg/mL in 50:50 pyridine:water).

QDs that were used for this work ranged from 3.45 to 4.09 nm and the size of the MPA capped QDs was 4.19 nm.

The absorbance and fluorescence emission spectra of the ZnPc complexes are shown in Fig. 2 (for TmTMPyZnPc and TmTPyZnPc) in a mixture of water and pyridine (50:50). In this solvent mixture, the ZnPc derivatives are less aggregated. Aggregation in MPc complexes is mainly due to a coplanar association of rings. This often results in the splitting and broadening of spectra, with a blue shifted peak at ~630 nm being due to the so-called "H" aggregates [55]. Addition of organic solvents normally breaks the aggregates, resulting in monomeric species, hence the pyridine:water solvent mixture was employed in this work. The ZnPc derivatives obeyed Beer's law for concentrations of 2.0×10^{-6} to 9×10^{-5} mol dm^{-3} in this solvent mixture. For the ZnPc derivative complexes (Fig. 2), the fluorescence emission spectra were mirror images of the absorption spectra. The ZnPc derivatives are positively charged while the QDs have a negatively charged surface by virtue of the carboxyl group at the terminal ends of the capping agent.

3.2. Interaction of quantum dots with TmTMPyZnPc (**4**)

It has been reported by Dayal et al. [36] as well as Sykora et al. [37] that QDs engage in various other processes in donor–acceptor

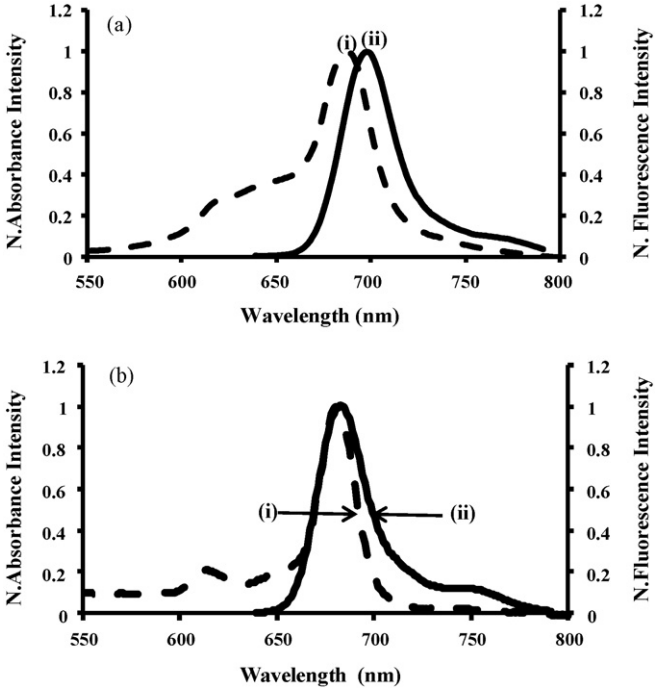

Fig. 2. Absorbance (i) and emission (ii) spectra of (a) TmTMPyZnPc ($\lambda_{excitation}$ = 615 nm) and (b) TmTPyZnPc ($\lambda_{excitation}$ = 620 nm) in 50:50 pyridine:water solution.

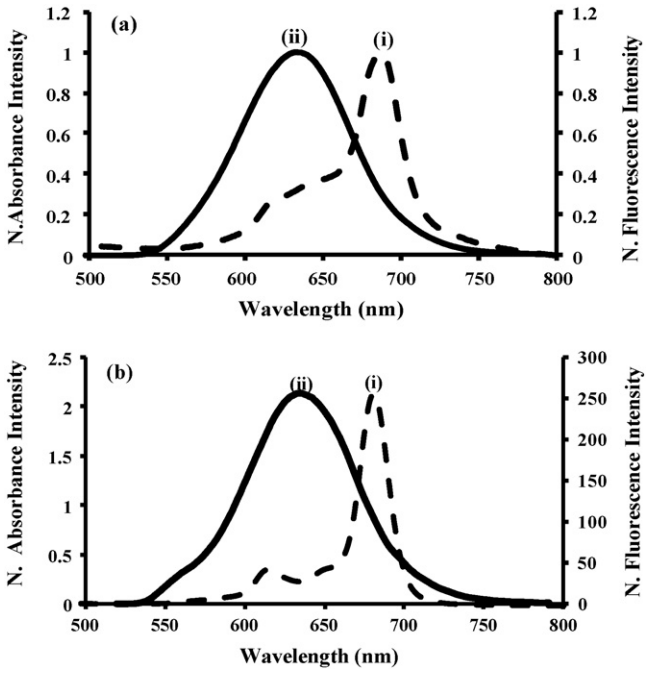

Fig. 3. Absorbance spectrum of ZnPc derivative (i) and emission spectrum of CdTe (MPA) (ii). (a) TmTMPyZnPc and (b) TmTPyZnPc in 50:50 pyridine:water solution ($\lambda_{excitation}$ = 500 nm).

systems other than FRET. We have recently reported on charge transfer between zinc-2,(3)-tetramethyltetraporphyrazine and CdTe QDs of different sizes capped with TGA and 2-ME [38]. The main deviation of our results from other charge transfer studies made with QDs was that charge transfer in this case occurred without photolysis.

Fig. 3 shows the extent of spectral overlap of QDs emission with absorption spectra of TmTMPyZnPc (**4**, Fig. 3a) and TmTPyZnPc (**6**, Fig. 3b). Both ZnPc derivative absorbances show good spectral overlap with QDs emission hence indicating a possibility of FRET. However, on addition of the QDs to the TmTMPyZnPc complex in the 50:50 pyridine:water solvent mixture, absorption and emission spectral changes shown in Fig. 4a and b, respectively were observed. These changes which consisted of a gradual collapse of the Q-band of the TmTMPyZnPc complex occurred without photolysis. The decrease in the Q-band of the ZnPc complex was accompanied by an increase in absorption between 450 and 600 nm, Fig. 4a, and this suggests ring reduction [56]. Reduction of the TmTMPyZnPc, observed in Fig. 4a, was confirmed by addition of chemical oxidants ($FeCl_3$ or bromine), which resulted in a slight regeneration of the Q-band (Fig. 4b). Thus, addition of QDs to TmTMPyZnPc (−2) resulted in the reduction of the latter complex to TmTMPyZnPc (−3), implying that there is electron transfer from the valence band of the QDs to the LUMO of the TmTMPyZnPc species. The lack of complete regeneration of the spectrum on addition of oxidizing agents suggests that it is not only reduction which occurs on addition of QDs to complex **4**. The shape of the spectra suggests the possibility of aggregation. Fig. 5 shows spectral changes observed on reduction of complex **4** with a chemical reducing agent (sodium borohydride). The spectra of the reduced species show similarity with Fig. 4a-ii. However, addition of oxidants to the solution formed after reduction using sodium borohydride, did not regenerate the spectra, suggesting aggregation. The aggregation could be a result of formation of S–S bonds between MPc molecules themselves or between MPc and the thiol groups on QDs. Spectral changes observed in Fig. 4 for TmTMPyZnPc (**4**, containing thio bridges) were not observed for TmTPyZnPc (**6**, containing oxo bridges). For the latter there were no

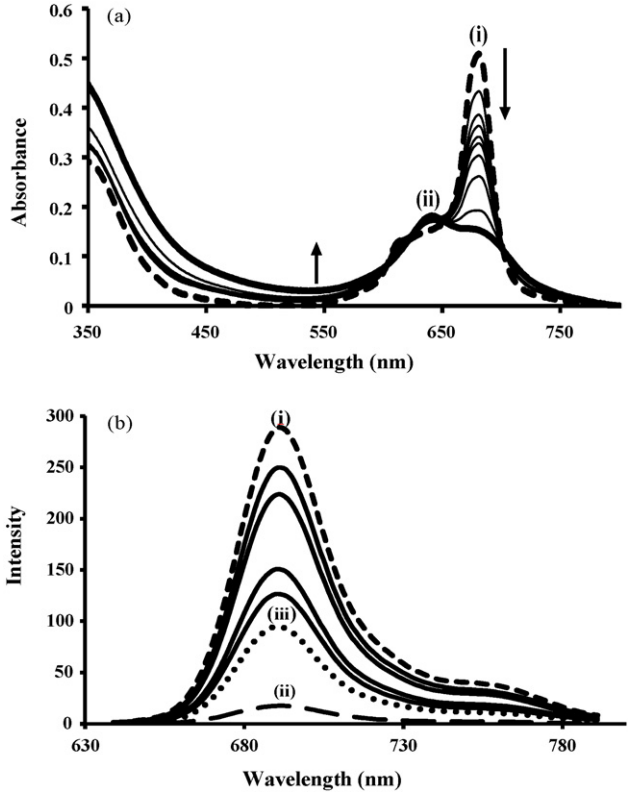

Fig. 4. Absorption spectral changes (a) for (i) TmTMPyZnPc only and (ii) final addition of QDs to TmTMPyZnPc and emission spectral changes (b) for (i) TmTMPyZnPc only, (ii) final addition of QDs to TmTMPyZnPc and (iii) addition of $FeCl_3$ to final TmTMPyZnPc-QD mixture ([TmTMPyZnPc] = 6.0×10^{-6} M, [QDs] = 1–10 μL of CdTe-TGA (4.09 nm) in 50:50 pyridine:water solution).

changes in the Q-band on addition of QDs (Fig. 6). The reason for different behavior of the two molecules in the presence of QDs could be due to the formation of S–S bonds which may encourage electron transfer in the case of TmTMPyZnPc. It is important to note that the spectral behavior similar to that of TmTMPyZnPc (**4**) was also observed for other positively charged MPc derivatives containing alkylthio-substituent groups.

Since the observed charge transfer from the QD to the TmTMPyZnPc (**4**) occurs without any driving force, this indicates that the overall charge transfer process is spontaneous. This being the case the activation energy (ΔG^*) for the process is zero ($\Delta G^* = 0$) [57]. Such behavior is usually observed in the barrierless regime according to Marcus theory and in this regime there is zero activation energy and the free energy of solvation (ΔG^0) is equal to a

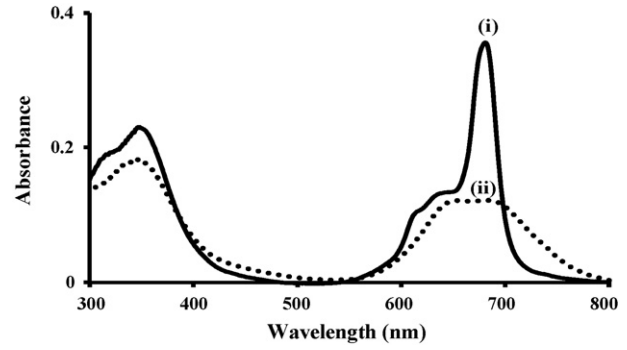

Fig. 5. Absorption spectral changes observed on addition of sodium borohydride to [TmTMPyZnPc] = 4.0×10^{-6} M. (i) Before and (ii) after addition of sodium borohydride.

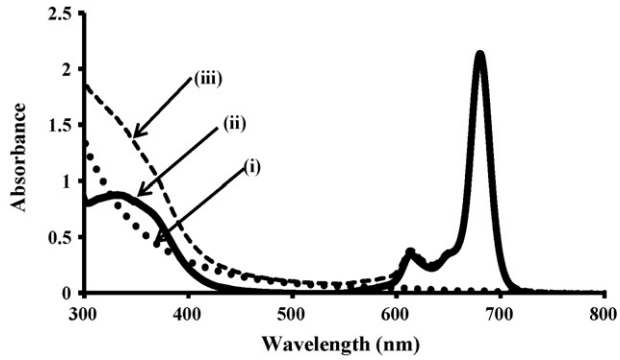

Fig. 6. Absorption of (i) CdTe (TGA), (ii) TmTPyZnPc and (iii) a mixture of TmTPyZnPc and QDs. Solvent: 50:50 pyridine:water solution ($\lambda_{excitation}$ = 500 nm).

large negative term of the solvent reorganization energy (λ). This free energy of solvation is required for the reorganization of solvent molecules around the donor and acceptor species and it involves an increase in entropy which will thus favor the electron transfer process [57,58].

3.3. Fluorescence quenching studies

The fluorescence emission spectra of CdTe QDs (1 mg/mL) in the presence of varying concentrations (0–5.3×10^{-6} M) of the TmTMPyZnPc (**4**) are shown in Fig. 7. The changes observed in Fig. 7a, are due to the quenching of the fluorescence of the CdTe QDs by the TmTMPyZnPc. The QDs fluorescence was found to decrease progressively with increasing concentration of TmTMPyZnPc. This quenching in fluorescence was used to estimate the binding constants (k_b) and the number of binding sites (n) using Eq. (2), Fig. 7b, with the results obtained listed in Table 1. The high values for k_b

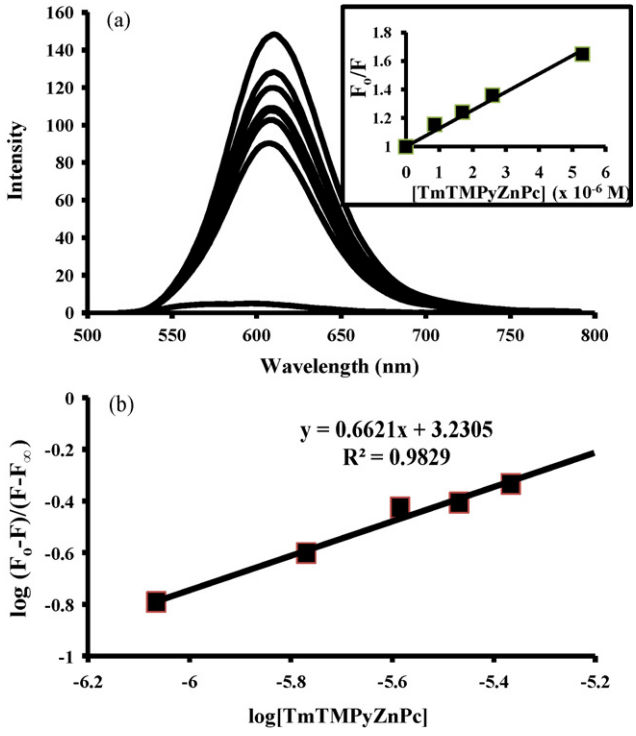

Fig. 7. (a) Variation of the photoemission spectra of CdTe-TGA QDs (1 mg mL^{-1}) in the presence of varying concentrations (0–5.3×10^{-6} M) of the TmTMPyZnPc (in 50:50 pyridine:water). Inset = plot of [TmTMPyZnPc] versus F_0/F. (b) Plot of log[TmTMPyZnPc] versus log[$(F_0 - F)/(F - F_\infty)$].

Table 1
Variation of the binding and quenching constants with the size of the CdTe (TGA) QDs (for TmTMPyZnPc in pyridine:water solution (1:1)).

Emission wavelength, λ (nm)	Size, D (nm)	k_b ($\times 10^{-3}$ M^{-1})	K ($\times 10^{-5}$ M^{-1})	n
570	3.45	0.54	0.99	0.57
590	3.59	1.20	1.09	0.62
610	3.94	1.70	1.28	0.66
620	4.09	56.7	1.32	0.93

indicate that there is a strong interaction between the QDs and TmTMPyZnPc. The interaction is expected to be electrostatic since the ZnPc derivatives are positively charged and the QDs are negatively charged by virtue of the terminal carboxyl moiety of the thiol capping groups used (TGA and MPA). The k_b values generally increased with increase in the size of the QDs, Table 1, and the value of n (number of binding sites on QDs) was found to be approximately one with all the different sizes of QDs as shown in Table 1. The number of binding sites remained practically the same with increase in size of the QDs while the binding constant k_b increased. Furthermore an increase in the concentration of the TmTMPyZnPc complex had no observable effect on the number of binding sites as they remained unchanged. We have recently shown that for porphyrazine molecules, the number of binding sites was two [38], hence showing the number of sites depends on the size and nature of the macrocycle.

The results suggest that one TmTMPyZnPc molecule attaches to one QD. The reasons for the binding of one TmTMPyZnPc molecule to each QD are not clear. Some factors that could influence the observed results may involve the tetra positive charge that the TmTMPyZnPc bears and the orientation of the bound ZnPc derivative molecules with regard to the QD. This is because the charge may cause repulsive forces between ZnPc derivative molecules so much that it becomes unfavorable to bind more than one TmTMPyZnPc molecule on one QD. One other reason may be attributed to steric effects.

The slopes of the plots of F_0/F against the concentration of the complex [ZnPc], Fig. 7a (inset), gave quenching constant (K) values for the fluorescence quenching of the QDs fluorescence with TmTMPyZnPc (Table 1). The linear plot in Fig. 7a (inset) confirms that the quenching equation (Eq. (3)) is obeyed. The values of K generally increased with increase in the size of the QDs as shown in Table 1.

3.4. Fluorescence quantum yields and energy transfer studies

Fluorescence quantum yield (Φ_F) values of the ZnPc derivatives (in the absence of QDs) are shown in Table 2 for excitation at 615 nm and were calculated by use of Eq. (4). TmTMPyZnPc (**4**) and TmTPyZnPc (**6**) gave Φ_F values of 0.11 and 0.17, respectively. The Φ_F values for the CdTe QDs in aqueous solution were calculated using Eq. (4) and are listed in Table 2. The fluorescence quantum yields (Φ_F) obtained for the QDs were fairly low and the values declined further in the presence of Pcs. This lowering of the Φ_F values of the QDs was anticipated in the presence of both MPc complexes due to the FRET occurring from the QD (donor) to the ZnPc molecules (acceptor) in their excited states as discussed below. There is also a chance of losing some of the energy through radiationless pathways. Consequently the quantum yields of the QDs in the QD-ZnPc mixtures are reduced.

Table 2
Photophysical parameters for TmTPyZnPc-CdTe-TGA QD interactions (in pyridine:water (1:1)).

ZnPc derivative	$\Phi_{F(ZnPc)}$ [a] ($\lambda_{excitation}$ = 615 nm)	Φ_Δ	Φ_{IC}	$\Phi_{T(ZnPc)}$ [b]	$\tau_{T(ZnPc)}$ [b] (μs)
TmTPyZnPc	0.17	0.66	0.05	0.78 (0.80)	30 (360)
TmTMPyZnPc	0.11	0.29	0.46	0.43	10

[a] QDs size: MPA = 4.19 nm and TGA = 4.09 nm. Φ_F values for quantum dots alone are CdTe-MPA = 0.21 and CdTe-TGA = 0.12. Φ_F^{Mix} values of quantum dots in the presence of TmTPyZnPc are CdTe-MPA = 0.17 and CdTe-TGA = 0.095.

[b] Values in brackets are for ZnPc derivatives in the presence of QDs.

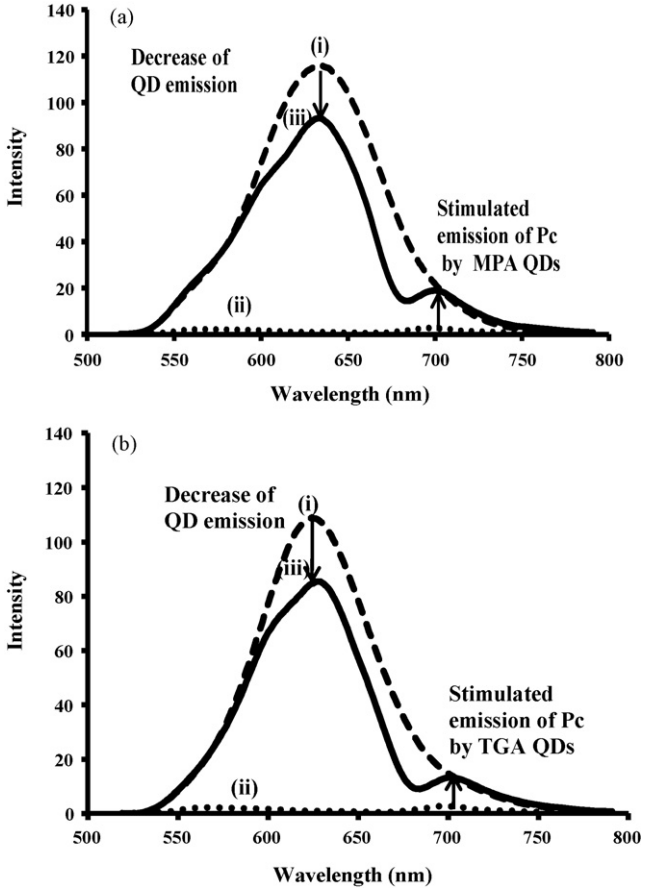

Fig. 8. Emission of (i) QDs alone, (ii) QDs in the mixture with TmTPyZnPc and (iii) TmTPyZnPc alone. (a) CdTe-MPA (4.19 nm) and (b) CdTe-TGA (4.09 nm) ($\lambda_{excitation}$ = 500 nm in 50:50 pyridine:water solution).

FRET was only observed between the CdTe (MPA and TGA capped QDs of the sizes 4.19 and 4.09 nm, respectively) and TmTPyZnPc, due to good spectral overlap with these larger sizes of QDs. The QDs were excited at 500 nm in the presence of TmTPyZnPc, where the MPc does not absorb and this resulted in a significant fluorescence of TmTPyZnPc as observed in Fig. 8a and b. Thus a clear transfer of energy (FRET) from the MPA or TGA-QDs to TmTPyZnPc was observed as suggested by the increase in the emission spectra of ZnPc derivative in the presence of QDs. There was insignificant emission by the TmTPyZnPc complex (in the absence of QDs) on excitation at 500 nm (Fig. 8a and b (curves ii)). The mode of interaction of the QDs with the TmTPyZnPc complex may have been electrostatic in nature since the quaternized ZnPc derivative (TmTPyZnPc) bears a tetra positive charge and the QDs bear a negative surface charge by reason of the terminal carboxyl moieties on the thiol capping groups.

The efficiency of FRET is known to be dependent on a number of parameters such as the spectral overlap term (J) estimated by overlapping QD emission with the absorbance of ZnPc derivatives shown in Fig. 3b. This extent of overlap has varied units and in this work the units used were in cm^6 [49]. The PhotochemCAD program gives J units as cm^6 following the use of ε_{ZnPc} in M^{-1} cm^{-1} and the wavelength λ in nm in Eq. (12). The Förster distance, R_0 (Å) is the

Table 3
Energy transfer parameters for TmTPyZnPc-CdTe-MPA QD interactions (in pyridine:water (1:1)).

Capping thiol	J ($\times 10^{-13}$ cm^6)	R_0 ($\times 10^{-10}$ m)	r ($\times 10^{-10}$ m)	*Eff*
TmTPyZnPc + CdTe-QD (MPA)	1.36	39.95	38.4	0.21
TmTPyZnPc + CdTe-QD (TGA)	1.17	35.47	44.20	0.21

critical distance between the donor and the acceptor molecule fluorophores for which efficiency of energy transfer is 50% [59,60], and the center-to-center separation distance (r, Å) between donor and acceptor chromophores. The J and R_0 values in this work were computed using PhotochemCAD [54] while the r values were calculated using Eq. (10) and are listed in Table 3.

J values are generally of the order of 10^{-14} cm^6 for porphyrin based molecules and the values obtained in this work were of the order of 10^{-13} cm^6 for the overlap between the QDs and TmTPyZnPc, as shown in Table 3. Table 3 shows that the overlap integral was reasonably large between the MPA or TGA-CdTe QDs emission and TmTPyZnPc absorbance. This is desirable since a greater value of J indicates good spectral overlap between the emission spectrum of the donor and the absorption spectrum of the acceptor giving an estimation of a good donor–acceptor oscillator match and hence a greater probability for FRET. This large J would most likely enhance the efficiency of energy transfer (FRET). The efficiency of FRET (*Eff*) values calculated using Eq. (9) from the QD to the ZnPc derivative (Fig. 8) are shown in Table 3. The values of r were fairly small indicating that the TmTPyZnPc is in close proximity to the donor (QDs) and thus there should be an ease of energy transfer (*Eff*) between the excited MPA or TGA capped QDs fluorophore and the TmTPyZnPc fluorophore.

3.5. Triplet quantum yields (Φ_T) and lifetime (τ_T) studies

A representative decay profile is shown in Fig. 9. The triplet decay curves for TmTPyZnPc alone and in the presence of QDs were similar. The values of Φ_T obtained by using Eq. (6) provide a measure of the fraction of absorbing molecules that undergo intersystem crossing (ISC) to the triplet state (Φ_T). The variation of Φ_T values of TmTPyZnPc only and TmTPyZnPc in the presence of the QDs are shown in Table 2. The Φ_T of the TmTPyZnPc complex both in the presence and the absence of QDs was quite high and this indicates that a considerable number of the ZnPc derivative molecules undergoes ISC. The Φ_T slightly increased in the presence of the quantum dots because they contain Cd and Te atoms which are heavy and thus encourage ISC. Our group previously reported a slight increase in the Φ_T values [33] for AlTSPc in the presence of CdTe QDs. However, the QDs do not seem to induce as great an increase in Φ_T values as would be expected on the basis of the heavy atom effect.

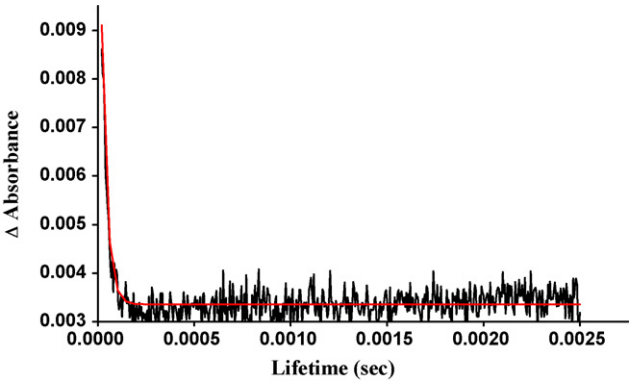

Fig. 9. A representative triplet decay curve for TmTPyZnPc (in 50:50 pyridine:water solution).

The triplet lifetimes (τ_T) of the TmTPyZnPc derivative showed a large increase in the presence of QDs. The higher τ_T value of the ZnPc derivative in the presence of QDs, does not correspond to the slight increase of the Φ_T values of the TmTPyZnPc derivative in the presence of QDs. High values of τ_T in the presence of QDs are desired as this would allow the excited ZnPc molecules to stay longer in the triplet state thus giving an opportunity for increased collisional and diffusional interactions between the ZnPc derivative molecules and ground state molecular oxygen ($^3O_2$) molecules. This would thus encourage a greater production of singlet oxygen ($^1O_2$) which is necessary in photosensitized reactions.

The internal conversion quantum yields (Φ_{IC}) were obtained through the use of Eq. (7). Internal conversion is one of the deactivation processes for a molecule in the excited state and it involves the radiationless transition between energy states of the same spin state. Φ_{IC} values indicate the extent of deactivation of excited state molecules with the result that the thermal energy of their surroundings increased. As shown in Table 2, the values of Φ_{IC} for TmTMPyZnPc (**4**) were greater than those of TmTPyZnPc (**6**) indicating that TmTMPyZnPc molecules are highly deactivated through radiationless transitions compared to their TmTPyZnPc counterparts. This could also account for the low Φ_F observed for TmTMPyZnPc.

3.6. Photochemical studies

3.6.1. Singlet oxygen quantum yields

Singlet oxygen quantum yield Φ_Δ is a measure of singlet oxygen generation and the Φ_Δ values were obtained using Eq. (8). Singlet oxygen is formed via interaction of the triplet state of a photosensitizer and ground state molecular (triplet) oxygen $O_2(^3\Sigma_g^-)$. Consequently the efficiency of singlet oxygen generation then depends on the triplet state quantum yield Φ_T and the triplet state lifetime τ_T. High Φ_T and τ_T would result in higher Φ_Δ values because of the increased molecular interactions between the photosensitizer in the triplet state and the ground state oxygen $O_2(^3\Sigma_g^-)$ causing formation of more singlet oxygen $O_2(^1\Sigma_g^-)$. Table 2 shows that the Φ_T for TmTPyZnPc is relatively high, and the value of Φ_Δ shown in the table is also high ($\Phi_\Delta = 0.66$) for this ZnPc derivative. However, TmTMPyZnPc had a low Φ_T and a high Φ_{IC} value both of which resulted in a low Φ_Δ ($\Phi_\Delta = 0.29$).

4. Conclusions

This work shows that CdTe QDs capped with TGA interact with TmTMPyZnPc differently compared to TmTPyZnPc. Spectral evidence suggests aggregation and charge transfer in the former. We propose that the difference in the two compounds is a result of the possibility of the formation of S–S bonds in the alkylthio substituted TmTMPyZnPc.

The QDs fluorescence is quenched by TmTMPyZnPc resulting in large quenching constants. Binding of TmTMPyZnPc to QDs occurs with one MPc molecule binding to the QDs of the size of 3.45–4.09 nm. The FRET interaction of CdTe quantum dots with TmTPyZnPc is observed due to the presence of a strong overlap between the emission of the MPA and TGA capped QDs (4.19 and 4.09 nm, respectively) and the absorption spectra of the TmTPyZnPc complex. The triplet quantum yields of TmTPyZnPc slightly increased in the presence of QDs and the lifetimes showed a large increase, hence making the combination of TmTPyZnPc and QDs potential candidates for applications as photosensitizers in PDT.

Acknowledgements

This work was supported by the Department of Science and Technology (DST) and National Research Foundation (NRF), South Africa through DST/NRF South African Research Chairs Initiative for Professor of Medicinal Chemistry and Nanotechnology as well as Rhodes University and Medical Research Council of South Africa. SM thanks DAAD foundation for a scholarship.

References

[1] J. Aldana, Y.A. Wang, X. Peng, J. Am. Chem. Soc. 123 (2001) 8844.
[2] J. Guo, W. Yang, C. Wang, J. Phys. Chem. B 109 (2005) 17467.
[3] A.L. Rogach, L. Katsikas, A. Kornowski, D. Su, A. Eychmüller, H. Weller, Ber. Bunsen. Phys. Chem. 100 (1996) 1772.
[4] A.M. Smith, S. Nie, Analyst 129 (2004) 672.
[5] A.C.S. Samia, S. Dayal, C. Burda, Photochem. Photobiol. 82 (2006) 617.
[6] H. Zhang, Z. Zhou, B. Yang, M. Gao, J. Phys. Chem. B 107 (2003) 8.
[7] A. Eychmuller, A.L. Rogach, Pure Appl. Chem. 72 (2000) 179.
[8] L. Qu, X. Peng, J. Am. Chem. Soc. 124 (2002) 2049.
[9] H. Zhang, L. Wang, H. Xiong, L. Hu, B. Yang, W. Li, Adv. Mater. 15 (2003) 1712.
[10] A. Shavel, N. Gaponik, A. Eychmuller, J. Phys. Chem. B 110 (2006) 19280.
[11] N. Kaji, M. Tokeshi, Y. Baba, Anal. Sci. 23 (2007) 21.
[12] I.L. Medintz, H.T. Uyeda, E.R. Goldman, H. Mattoussi, Nat. Mater. 4 (2005) 435.
[13] A.C.S. Samia, X. Chen, C. Burda, J. Am. Chem. Soc. 125 (2003) 15736.
[14] J.K. Jaiswal, H. Mattoussi, J.M. Mauro, S.M. Simon, Nat. Biotechnol. 21 (2003) 47.
[15] Y. Zhang, J. He, P. Wang, J. Chen, Z. Lu, D. Lu, J. Guo, C. Wang, W. Yang, J. Am. Chem. Soc. 128 (2006) 13396.
[16] M.N. Rhyner, A.M. Smith, X. Gao, H. Mao, L. Yang, S. Nie, Nanomedicine 1 (2006) 2091.
[17] X. Gao, W.C.W. Chan, S. Nie, J. Biomed. Opt. 7 (2002) 532.
[18] M. Achermann, M.A. Petruska, D.D. Koleske, M.H. Crawford, V.I. Klimov, Nano Lett. 6 (2006) 1396.
[19] R. Bakalova, H. Ohba, Z. Zhelev, T. Nagase, R. Jose, M. Ishikawa, Y. Baba, Nano Lett. 4 (2004) 1567.
[20] X. Gao, S. Nie, Trends Biotechnol. 21 (2003) 371.
[21] M. Zhou, I. Ghosh, Pept. Sci. 88 (2006) 325.
[22] R.E. Bailey, A.M. Smith, S. Nie, Physica E 25 (2004) 1.
[23] S. Kim, Y.T. Lim, E.G. Soltesz, A.M. De Grand, J. Lee, A. Nakayama, J.A. Parker, T. Mahaljevic, R.G. Laurence, D.M. Dor, L.H. Cohn, M.G. Bawendi, J.V. Frangioni, Nat. Biotechnol. 22 (2004) 93.
[24] E.R. Goldman, I.L. Medintz, H. Mattoussi, Anal. Bioanal. Chem. 384 (2006) 560.
[25] J.K. Jaiswal, E.R. Goldman, H. Mattoussi, S.M. Simon, Nat. Methods 1 (2004) 73.
[26] A.L. Rogach, Mater. Sci. Eng. B 69–70 (2000) 435.
[27] N. Gaponik, V.D. Talapin, K. Hoppe, E.V. Shevchenko, A. Kornowski, A. Eychmuller, H. Weller, J. Phys. Chem. B 106 (2002) 7177.
[28] S. Gaspard, T.H. Tran-Thi, J. Chem. Soc., Perkin Trans. II (1989) 383.
[29] L. Stryer, Annu. Rev. Biochem. 47 (1978) 819.
[30] L. Lankiewicz, J. Malicka, W. Wiczk, Acta Biochim. Pol. 44 (1997) 477.
[31] D. Sokol, X. Zhang, P. Lu, A. Gewirtz, Proc. Natl. Acad. Sci. U.S.A. 35 (1998) 11538.
[32] M. Idowu, J.-Y. Chen, T. Nyokong, New J. Chem. 32 (2008) 290.
[33] J. Ma, J.-Y. Chen, M. Idowu, T. Nyokong, J. Phys. Chem. B 112 (2008) 4465.
[34] M. Idowu, E. Lamprecht, T. Nyokong, J. Photochem. Photobiol. A: Chem. 197 (2008) 273.
[35] S. Dayal, C. Burda, J. Am. Chem. Soc. 129 (2007) 7977.
[36] S. Dayal, Y. Lou, A.C.S. Samia, J.C. Berlin, M.E. Kenney, C. Burda, J. Am. Chem. Soc. 128 (2006) 13974.
[37] M. Sykora, M.A. Petruska, J.A. Acevedo, I. Bezel, T.J. Meyer, V.I. Klimov, J. Am. Chem. Soc. 128 (2006) 9984.
[38] S. Moeno, M. Idowu, T. Nyokong, Inorg. Chim. Acta 361 (2008) 2950.
[39] N. Sehlotho, M. Durmus, V. Ahsen, T. Nyokong, Inorg. Chem. Commun. 11 (2008) 279.
[40] W. Chidawanyika, A. Ogunsipe, T. Nyokong, New J. Chem. 31 (2007) 377.
[41] N. Saydan, M. Durmuş, M.G. Dizge, H. Yaman, A.G. Gürek, E. Antunes, T. Nyokong, V. Ahsen, J. Porphyrins Phthalocyanines, in press.
[42] W.W. Yu, L. Qu, W. Guo, X. Peng, Chem. Mater. 15 (2003) 2854.
[43] S. Lehrer, G.D. Fashman, Biochem. Biophys. Res. Commun. 23 (1966) 133.
[44] S.M.T. Nunes, F.S. Sguilla, A.C. Tedesco, Braz. J. Med. Biol. Res. 37 (2004) 273.
[45] D.M. Chipman, V. Grisaro, N. Sharon, J. Biol. Chem. 242 (1967) 4388.
[46] S. Fery-Forgues, D. Lavabre, J. Chem. Ed. 76 (1999) 1260.
[47] A. Ogunsipe, J.-Y. Chen, T. Nyokong, New J. Chem. 28 (2004) 822.
[48] R.F. Kubin, A.N. Fletcher, J. Lumin. 27 (1982) 455.
[49] J.R. Lakowiecz, Principles of Fluorescence Spectroscopy, 2nd ed., Kluwer Academic/Plenum Publishers, New York, 1999.
[50] A. Harriman, M.C. Richoux, J. Chem. Soc., Faraday Trans. II 76 (1980) 1618.
[51] S. Maree, T. Nyokong, J. Porphyrins Phthalocyanines 5 (2002) 782.
[52] R. Bonnett, Chemical Aspects of Photodynamic Therapy, Gordon and Breach Science, Canada, 2000.
[53] A. Ogunsipe, D. Maree, T. Nyokong, J. Mol. Struct. 650 (2003) 131.
[54] H. Du, R.A. Fuh, J. Li, L.A. Corkan, J.S. Lindsey, Photochem. Photobiol. 68 (1998) 141.
[55] H. Engelkamp, R.J.M. Nolte, J. Porphyrins Phthalocyanines 4 (2000) 454.
[56] M.J. Stillman, T. Nyokong, in: C.C. Leznoff, A.B.P. Lever (Eds.), Phthalocyanines: Properties and Applications, vol. 1, VCH, New York, 1989 (Chapter 3).
[57] A.J. Bard, L.R. Faulkner, Electrochemical Methods Fundamentals and Applications, 2nd ed., John Wiley & Sons, New York, 2001 (Chapter 3).
[58] R.A. Marcus, J. Chem. Phys. 24 (1956) 966.
[59] J.S. Hsiao, B.P. Krueger, R.W. Wagner, T.E. Johnson, J.K. Delaney, D.C. Mauzerall, G.R. Fleming, J.S. Lindsey, D.F. Bocian, R.J. Donohoe, J. Am. Chem. Soc. 118 (1996) 11181.
[60] T. Forster, Disc. Faraday Soc. 27 (1959) 7.